www.czasopisma.pan.pl PAN POLSKA AKADEMIA NAUK www.journals.pan.pl

Arch. Metall. Mater. **64** (2019), 1, 143-151

DOI: 10.24425/amm.2019.126230

I. LYASOTA*#, Ł. SARNIAK**, P. KUSTRA***

ACOUSTIC EMISSION SNALYSIS OF THE PLASTIC DEFORMATION STAGES OF DEGRADED LOW-CARBON STEEL AFTER LONG-TERM OPERATION IN THE OIL REFINING AND PETROCHEMICAL PROCESSING

This paper presents results obtained from a laboratory investigation conducted on material from a pressure vessel after long-term operation in the oil refinery industry. The tested material contained structural defects which arose from improper heat treatment during steel plate manufacturing. Complex tensile tests with acoustic emission signal recording were conducted on both notched and unnotched specimens. The detailed analysis of different acoustic emission criteria allowed as to detect each stage of plastic deformation and microstructural damage processes after a long-term operation, and unused carbon steels during quasi-static axial tension testing. The acoustic emission activity, generated in the typical stages of material deformation, was correlated by microscopy observations during the tensile test. The results are to be used as the basis for new algorithms for the assessment of the structural condition of in-service pressure equipment.

Keywords: monitoring, low carbon steel, plastic deformation, acoustic emission, refinery industry

1. Introduction

Different types of pressure equipment are widely used in oil refining and petrochemical processing. A lot of these were made from carbon steels and have been used for a few decades. Long-term operation under extreme conditions causes defect initiation and growth in the microstructure of the equipment materials. The defects, which grow due to work loads, may damage the entire structure and may lead to the failure of the entire industrial unit.

Consequently, the development of new non-destructive evaluation methodologies which allow the assessment of the condition of materials comprising the pressure equipment after long-term operation in the refinery industry is very important. The development of non-destructive evaluation (NDE) methodologies is possible as a result of complex destructive laboratory tests combining different experimental techniques. This research was conducted in order to study the influence of microstructural degradation of low carbon steel on acoustic emission (AE) generated by plastic deformation and fracture processes during quasi-static axial tension. The tested material was cut out from a pressure vessel shell which had been in operation for many years in the oil refining processing. The tensile tests of unnotched and notched flat specimens with AE signals recording were performed. Microstructural damage processes were correlated by in situ examinations with use of optical microscopy (OM). The results of the studies will be used to develop AE criteria for assessing the condition of in-service pressure vessel material. The

investigations presented in this paper were supported as a part of the project of LIDER VII Programme financed by the National Centre for Research and Development of Poland.

The AE behaviour in structural materials during deformation, fracture and other processes continues to be systematically examined with advances in AE measuring systems and signal processing methods. Extensive studies of AE behaviour under tension of Armco (pure) iron and ultra-low carbon steels [1-3] as well as two-phased (ferrite-pearlite) low carbon steels (<0.2%C) [4-14] unnotched specimens were conducted.

In the case of plastic deformation of Armco iron specimens, AE is generated starting at the yield drop, followed by Lüders-band propagation and macroscopic strain localisation associated with necking followed by crack nucleation and propagation. The AE signals from both Lüders instability and necking with a significant shift of the power spectral density towards low frequencies are observed [1]. The AE technique also allows for sensitive detection of the deformation and damage mechanisms of ultra-low carbon steels (<0.08%C) in early loading stages [2,3].

As a result of the tensile process of structural low carbon steel (i.e. Q235, Q345 steels), AE signals with the typical features at different stages of loading are generated [4-12]. The beginning of plastic deformation is detected by AE in two stages [7]. At the early stage of plastic deformation (the microyield stage), AE is generated by dislocation activity at grain boundaries; a rapid increase of AE activity is then observed after massive plastic deformation at yield due to intense motion of slip bands [7].

* CRACOW UNIVERSITY OF TECHNOLOGY, FACULTY OF MECHANICAL ENGINEERING, AL. JANA PAWŁA II, 31-864 KRAKOW, POLAND
** WARSAW UNIVERSITY OF TECHNOLOGY, FACULTY OF MATERIALS SCIENCE AND ENGINEERING, 141 WOLOSKA STR., 02-507 WARSZAWA, POLAND
*** AGH UNIVERSITY OF SCIENCE AND TECHNOLOGY, FACULTY OF METALS ENGINEERING AND INDUSTRIAL COMPUTER SCIENCE, AL. MICKIEWICZA 30, 30-059 KRAKOW, POLAND
# Corresponding author: igor.lyasota@mech.pk.edu.pl

According to [4,12], the first low-energy AE signals can be attributed to the dislocation multiplication and unpinning from the Cottrell atmosphere or dislocation tangling, while the latter AE signals may be generated by the simultaneous motion of high-density dislocations during Lüders-band propagation. Generally, the activity of AE increases near the yield point and reaches maximum at the beginning of plastic deformation, but then the activity decreases significantly (exponentially [5]) with further straining when the material reaches the initial fracture region [4,7,10,14]. The related AE behaviour and deformation properties have been analysed [7]. Two typical AE signals were obtained: the lower amplitude and higher energy AE signals in the yielding stage and the higher amplitude and lower energy AE signals in micro-plastic deformation and the strain-hardening stage. The AE signals show a waveform with a long rise time and low amplitude. The peak of the signal frequency spectrum occurs at the relatively high frequencies of 170 kHz [12] and 270-300 kHz [11].

According to [12,13], the grain size of low carbon steel also influences the AE generated by plastic deformation and cracking. AE activity from coarse-grained microstructure is higher than the activities from the normalised microstructure. The coarse-grained microstructure is more prone to damage than the heat-treated (normalised) specimen material, which is stable [13]. In the case of tensile tests of low carbon steel with different martensite morphologies and volume fractions (0.3-0.8), the AE energy rate and amplitude exhibits two peaks: the first peak is located around the yield point [15, 16] and the second peak is in the post-yielding stage [12]. The amplitude of the AE signals is different for each deformation stage. In addition to the low-amplitude AE signals which were generated around the yield point there are many AE events which occur at amplitudes higher that 50 dB (in reference to 0 dB at 1 μV input). High amplitude signals are characteristic of the second AE activity peak. Both AE amplitude and the number of events increase if the volume fraction of martensite increases. Some AE sources were recognised by [12,15,16] as being: ferrite deformation, the martensite phase fracture and ferrite-martensite interface decohesion. AE signals with a short rise time and a higher amplitude of waveforms are generated by ferrite-martensite interfacial cracking. The frequency range of AE signals from ferrite deformation is 150-175 kHz and the range for martensite is between 520 and 700 kHz [15, 16]. AE signals generated by ferrite-martensite decohesion occur in the frequency range 110-130 kHz [12, 15, 16].

The analysis of fracture mechanisms during three-point static bending test of specimens, machined from 20GL (G21Mn5) grade steel with a different heat-treatments was prepared by authors [17]. These investigations allowed to develop the system for damage monitoring of train solebars using AE method. Quantitative analysis of damage processes, obtained in AE measurements, was also carried out by authors [18,19]. The necessary conditions for the quantitative evaluation of fracture process by AE were shown. Examples were considered of quantitative AE measurements in hydrogen embrittlement of 40Kh2GMF steel [18]. Acoustic emission method has been also used for analysing the mechanisms and kinetics of fracture processes and classifying the formed cracks. This has made it possible to determine the structural causes of the decrease in plasticity and fracture toughness among others for G7Kh2MF steel [19].

As the review of existing literature demonstrates, the AE method is highly sensitive to steel deformation and fracture during tensile testing. The AE method allows attributing different AE signals to various deformation and damage mechanisms in the structure materials, such as: dislocation glide, twinning, crack initiation and propagation. It is also worth noting that not many publications are dedicated to this topic.

2. Materials and Methods

Two materials were tested in this study. The first material – St3S hot-rolled low-carbon steel plate – was obtained from a crude oil distillation column shell which had had fifty years of operation in a petroleum refinery. The second material was unused S235 grade steel plate with a similar chemical composition as the used material. The new material was tested in order to conduct a comparative analysis. The chemical compositions and mechanical properties of the tested materials are presented in Tables 1 and 2.

TABLE 1

Chemical composition of the tested St3S and S235 low-carbon steels [20,21]

Material	Chemical elements, [%]				
	C	Mn	Si	P	S
St3S	0.14-0.22	0.40-0.65	0.12-0.35	Max. 0.080	Max. 0.060
S235	Max. 0.17	Max. 1.40	—	Max. 0.035	Max. 0.035

TABLE 2

Mechanical properties of the tested St3S and S235 low-carbon steels [20,21]

Material	R_e, MPa	R_m, MPa	A_5, %
St3S	220-240	380-470	21-27
S235	Min. 223	Min. 360	Min. 26

Microscopic observations of the metallographic section of St3S steel by OM showed an overheated coarse-grained ferrite-pearlite microstructure (Fig. 1a). These changes to the microstructure morphology arose due to material overheating in the Ar3 and Ar1s temperature range and could not have been caused by the operating conditions of the distillation column. These microstructural defects arose from improper normalisation treatment after hot rolling during steel plate manufacturing. Steel with such a microstructure has a tendencies for brittle fracturing, reduced impact strength and mechanical properties such as R_e, R_m during tensile test.

Metallographic examination of unused S235 grade steel plate showed a ferrite-pearlite microstructure that is typical

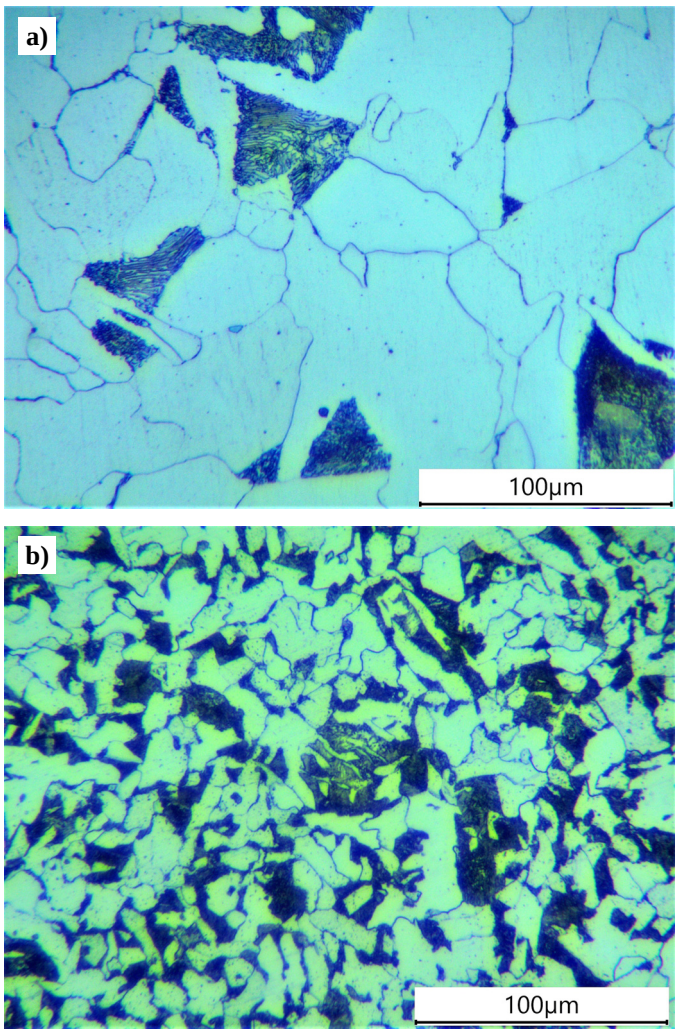

Fig. 1. The microstructure of St3S steel (a) and S235 steel (b), magnification 500×

for this steel (after normalising treatment) (Fig. 1b). The microstructures of both materials contain non-metallic inclusions (manganese and iron sulphides) with shapes orientated in line with the direction of rolling. The inclusions were caused by the steel production technology.

The static tensile tests with AE recording were conducted on both unnotched and notched flat specimens (Fig. 2a) machined from each material. The unnotched specimens were designated as 'St3S-unnotched', 'S235-unnotched' and notched samples were designated as 'St3S-notched', 'S235-notched'. The notch from the one side of the specimen was made using the electroerosion method (tip radius – 0,05 mm). The work zones of the specimens (flat side of specimens between shoulders) were polished and etched with the use of portable metallographic techniques.

The specimens were axially loaded on a testing machine with hydraulic serrated grips. As shown in Fig. 2b, the AE signals were recorded using VS150-M and VS75-V type resonance sensors (resonance frequency of 150 kHz and 75 kHz) with external preamplifiers 34 dB. The acquisition threshold was 35 dB. The calibration of AE-channels was conducted with the use of the 2H/0.5 mm Hsu-Nielsen source according to the PN-EN 13554:2011 standard [22].

3. Results and discussion

3.1. The AE generated during unnotched specimens tension

The representative tensile test results, such as stress-displacement curves with AE signal parameter distribution and material microstructure images for each stage of unnotched

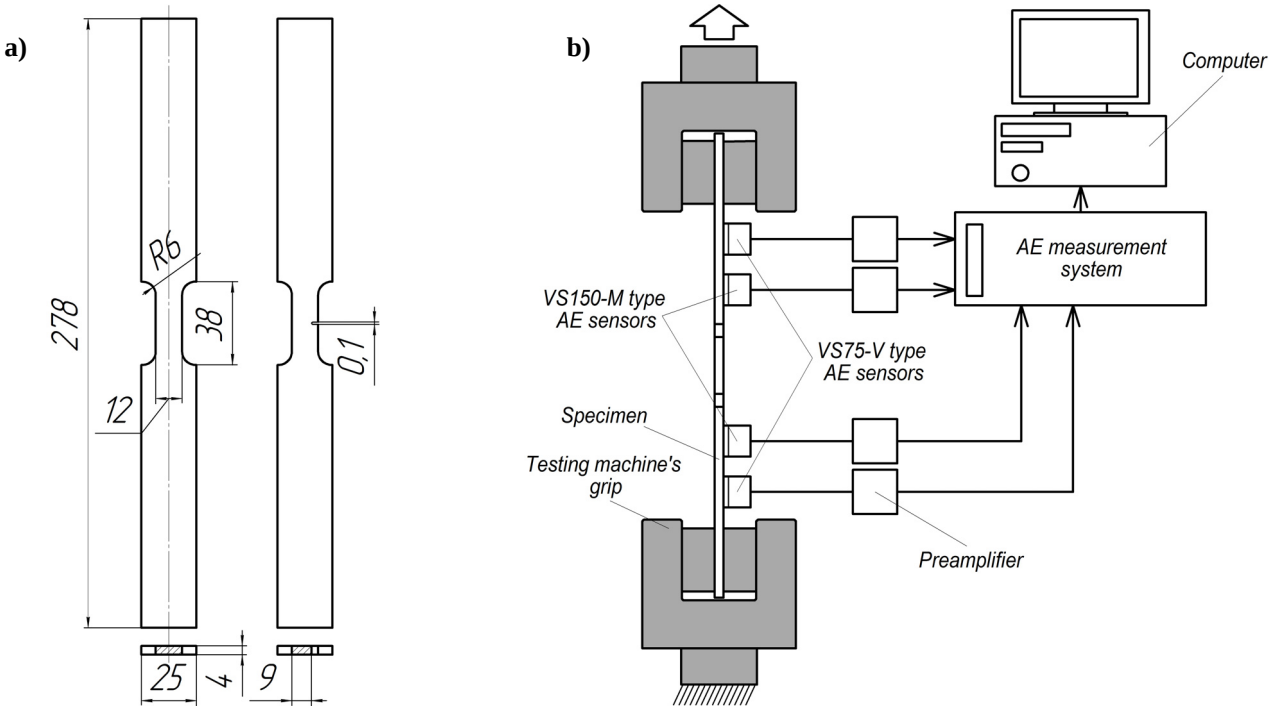

Fig. 2. Technical drawing of tested specimens (a) and diagram of the testing station (b)

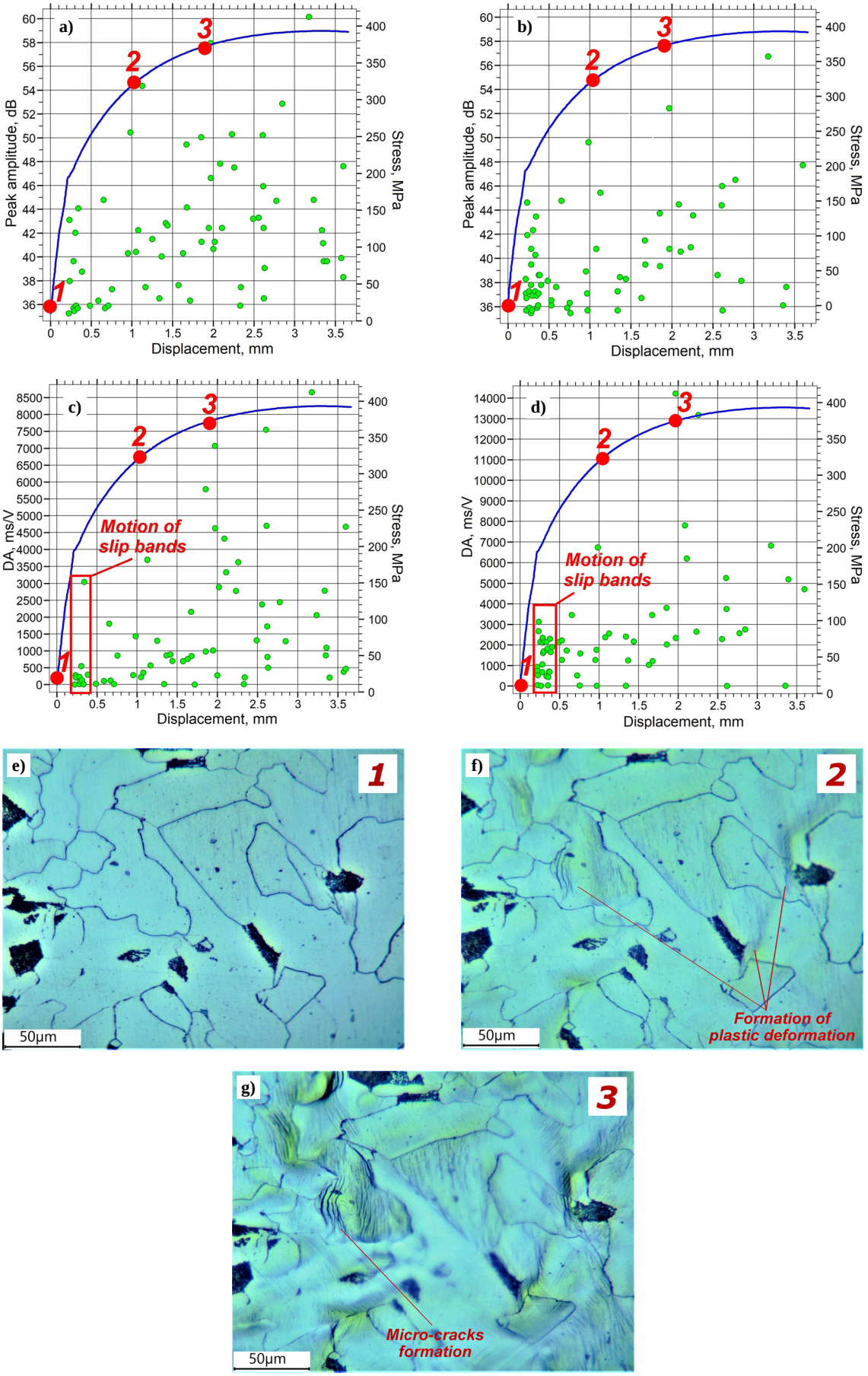

Fig. 3. Stress-displacement curves of 'St3S-unnotched' type specimen with AE signal amplitude (a, b) and *DA* signal parameter (c, d) distributions for type VS150-M sensors (a, c) and type VS75-V sensors (b, d) as well as material microstructure images (e-g) for different stress levels, magnification 400×

specimen tension, are shown in Figures 3 and 4. Only AE signals located in the work zones of specimens were taken into account. The results of conducted analysis demonstrated significant differences in the parameters of AE signals generated during the tensile testing of degraded and new material.

The rapid increase of AE activity with burst signal peak amplitudes of approx. 45-60 dB (Fig. 3a,b and Fig. 4a,b) was recorded by all AE channels during the tensile tests of materials designated as 'St3S-unnotched' and 'S235-unnotched'. The highest activity of the DA parameter value (DA = the duration/the maximum amplitude [23]) was also noted when the materials reached the yield point (Fig. 3c,d and Fig. 4c,d). The DA values for signals recorded by channels with a type VS75-V sensor were much higher than those recorded by type VS150-M sensors. It was confirmed that AE sensors with a resonance frequency of 75 kHz are more sensitive with regard to the plastic deformation of steel. According to [1,4,7,12] AE at the early stage of plastic deformation, preceded by a yield point, is generated by dislocation movement at grain boundaries. A rapid increase of AE activity is then observed after massive plastic deformation – intensive development of slip bands (shear deformation on multiple slip planes) in ferrite grains as well as during Lüders-band propagation in the lower yield point. The DA parameter allowed separation of the AE-signals generated by dislocation movement near the yield point (Fig. 3c,d and Fig. 4c,d).

The processes of intensive slip band formation in ferrite grains inhibit material deformation after the yield point (dislocation blocking); this is the start of the strain hardening stage. In this stage, the dislocations accumulate, interact with one another, and serve as obstacles for their movement. This leads to a change in the deformation mechanism from a strong dislocation motion to a short-range motion. The strain hardening process requires a higher stress level than slip bands. The linear plastic deformation zones are formed in ferrite grains of low carbon steel as a result of the strain hardening processes. These zones can already be observed with the use of OM (Fig. 3f) during the tensile test. The decrease of AE activity was observed during the strain hardening stage (Fig. 3a,b and Fig. 4a,b). It was found that the plastic deformation of overheated coarse-grained St3S steel clearly generates lower AE activity than new material.

The next stage was the micro-crack formation process in the linear plastic deformation zones of ferrite grains (Fig. 3g). These processes started after reaching the maximum load. Each micro-cracking process generates a single burst signal with peak amplitudes of approx. 50-60 dB. The growth and linkage of micro-cracks as well as macro-cracks development occurs on the final fracture stage when load decreases are observed.

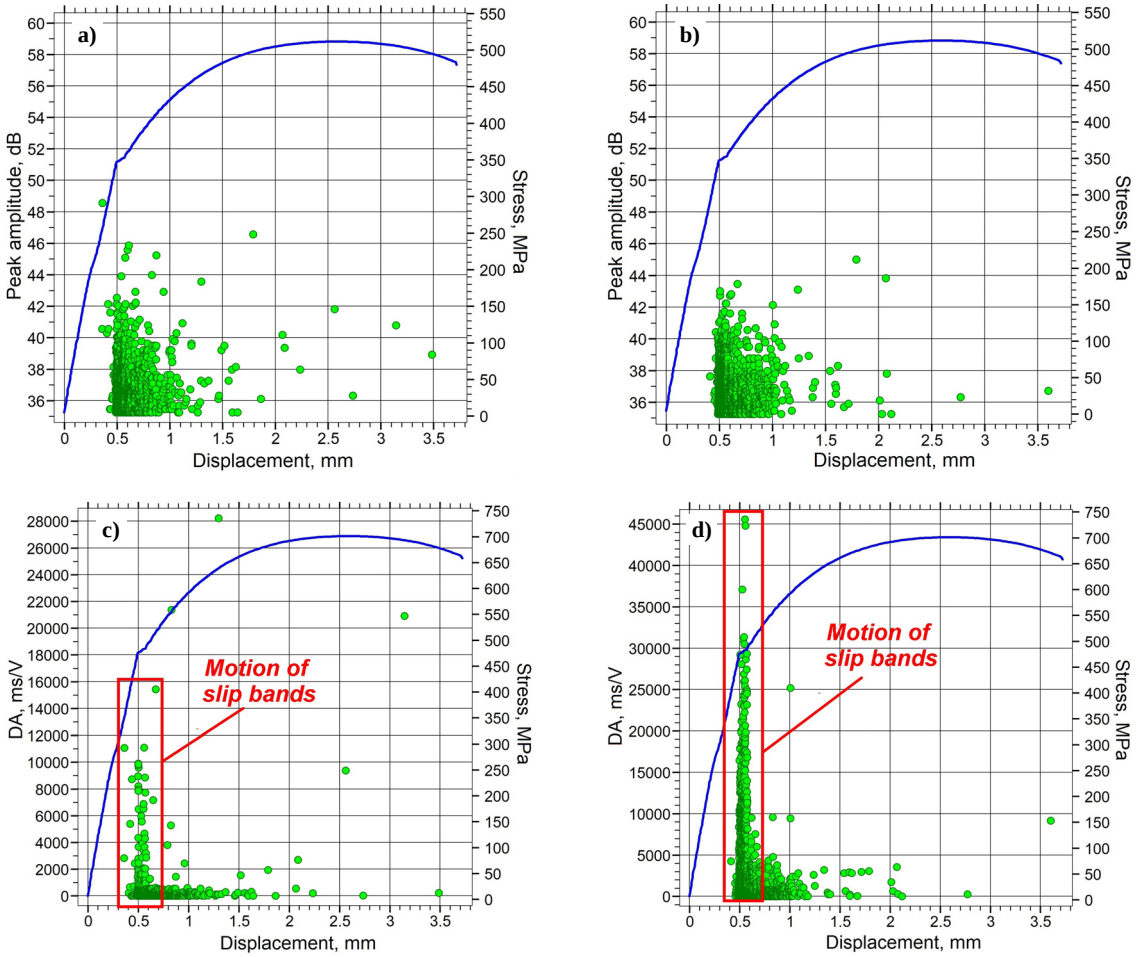

Fig. 4. Stress-displacement curves of 'S235-unnotched' type specimen with AE signal amplitude (a, b) and *DA* signal parameter (c, d) distributions for type VS150-M sensors (a, c) and type VS75-V sensors (b, d)

3.2. The AE generated during notched specimens tension

Example results of notched specimen tension tests such as stress-displacement curves with AE signal parameter distribution are shown in Figs. 5 and 6. The analysis of results demonstrated significant differences in AE behaviour which were generated during the tensile testing of two specimen types. The AE signals with high values of burst peak amplitudes were recorded almost from the beginning of the tensile test of notched specimens. By contrast, a rapid increase of AE activity was observed only near the yield point in the case of the unnotched samples (Figs. 3 and 4).

The detailed analysis of AE signal parameters (max amplitude distributions and Historic Index parameter – MONPAC criterion [24]) allowed us to identify each stage/mechanism of deformation and fracture processes during the tensile test of carbon steel notched specimens (Figs. 5 and 6). The first stage was the formation of the plastic deformation area in the material near the notch tip (Fig. 5c,d and Fig. 6c,d). The plasticising in the notch tip of the St3S steel specimens occurred after exceeding a stress value approx. 40 MPa (in the stress-displacement curve). For S235 steel specimens, this value was approx. 60 MPa. This fact has been validated by in situ observations of material microstructure changes in the notch tip with the use of OM. In addition, the finite element method (FEM) calculations

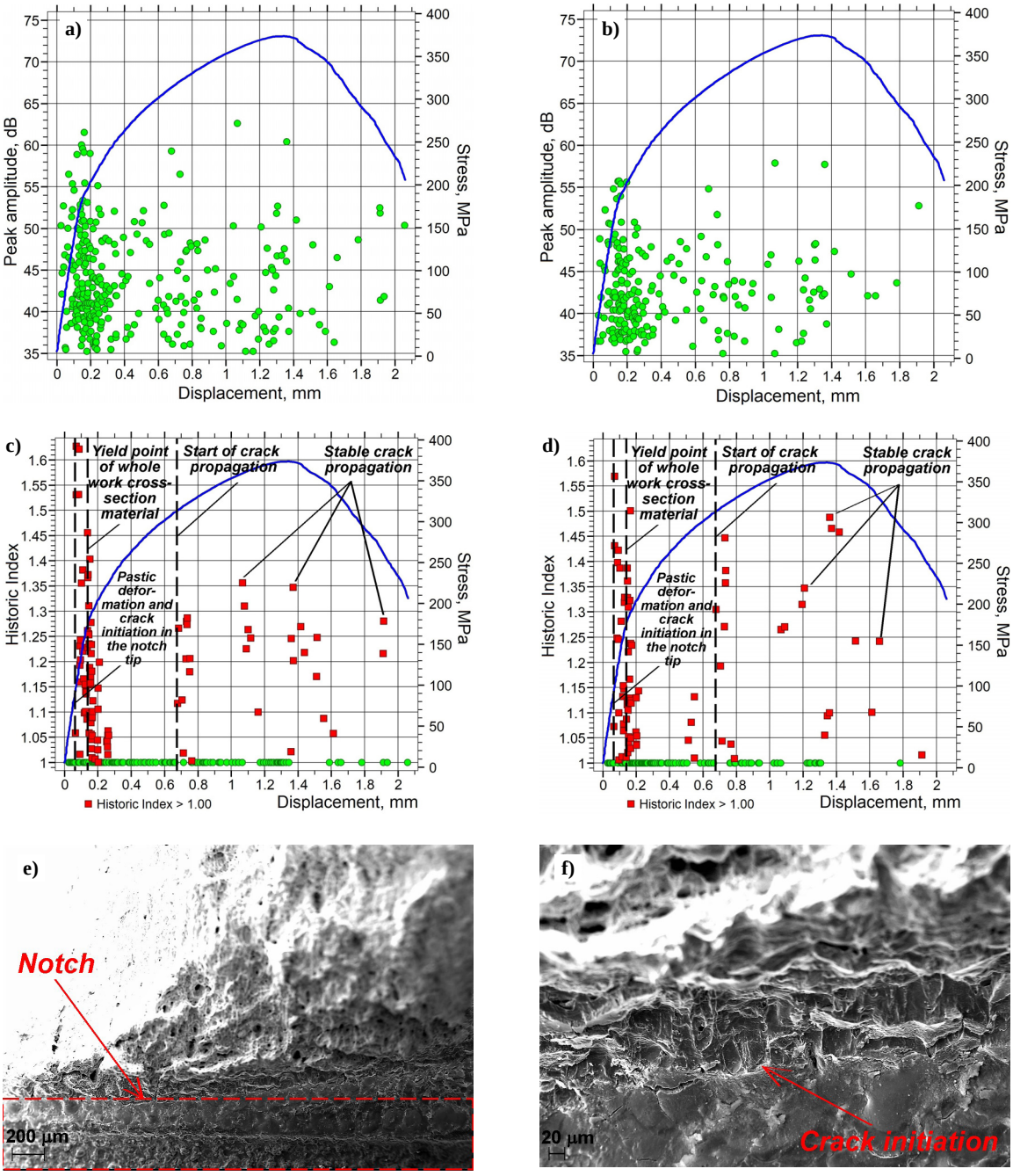

Fig. 5. Stress-displacement curves of 'St3S-notched' type specimen with AE signal amplitude (a, b) and Historic Index signal parameter (c, d) distributions for type VS150-M sensors (a, c) and type VS75-V sensors (b, d) as well as fractography images (e, f)

(with nonlinear analyses) showed a stress concentration in the specimen notch tip (Fig. 6e). The values of these stresses exceed material yield strength (for S235 steel – R_e = 340 MPa) for the abovementioned load conditions. The process of plastic deformation zone formation generated high AE activity (practically from the beginning of loading the sample). The next stage of the fracture process was crack initiation at the notch tip, which was also confirmed by the FEM calculations and fractography investigations with the use of scanning electron microscopy (Fig. 5e,f). Crack initiation caused an active increase in the AE parameter values. The burst peak amplitudes of the AE signals reached their maximum values of approx. 60-70 dB at this point. For example, in the case of S235 steel, the crack was developed after exciting approx. 170 MPa on the stress-displacement curve (Fig. 6a-d). This load exceeds of the material ultimate strength (for S235 steel – R_m = 545 MPa) at the notch tip according to the FEM analysis (Fig. 6f).

The materials plastic deformation in the work cross-section of specimens (yield point in the stress-displacement curves) was observed in the next stage of the material damage process. The plastic deformation and strain hardening of material in the work cross-section served as obstacles for crack propagation.

Next, there was rapid crack growth after material strain hardening. The increase of AE activity was also noted when the crack propagation started (Fig. 5a-d and Fig. 6a-d). The crack propagation was gradual. The plastic deformation zones around crack tip were formed in the intervals between 'crack's sudden jumps'. These processes generated AE signals with maximum amplitudes of approx. 60-65 dB. The last stage was the critical propagation of the crack.

It was confirmed the known fact that AE sensors with a resonance frequency of 75 kHz were more sensitive with regard to plastic deformation of steel, but sensors with a frequency of 150 kHz had a higher sensitivity to crack initiation and propagation processes.

4. Conclusions

1. The AE method allowed the detection of the early stages of plastic deformation and damage processes in long-term operation St3S and unused S235 carbon steels during quasi-static axial tension testing of unnotched and notched specimens.
2. The AE generated by the damage processes of steel was correlated with *in situ* microstructural observation with optical microscopy as well as fractography examinations and FEM simulations of stress/strain fields.

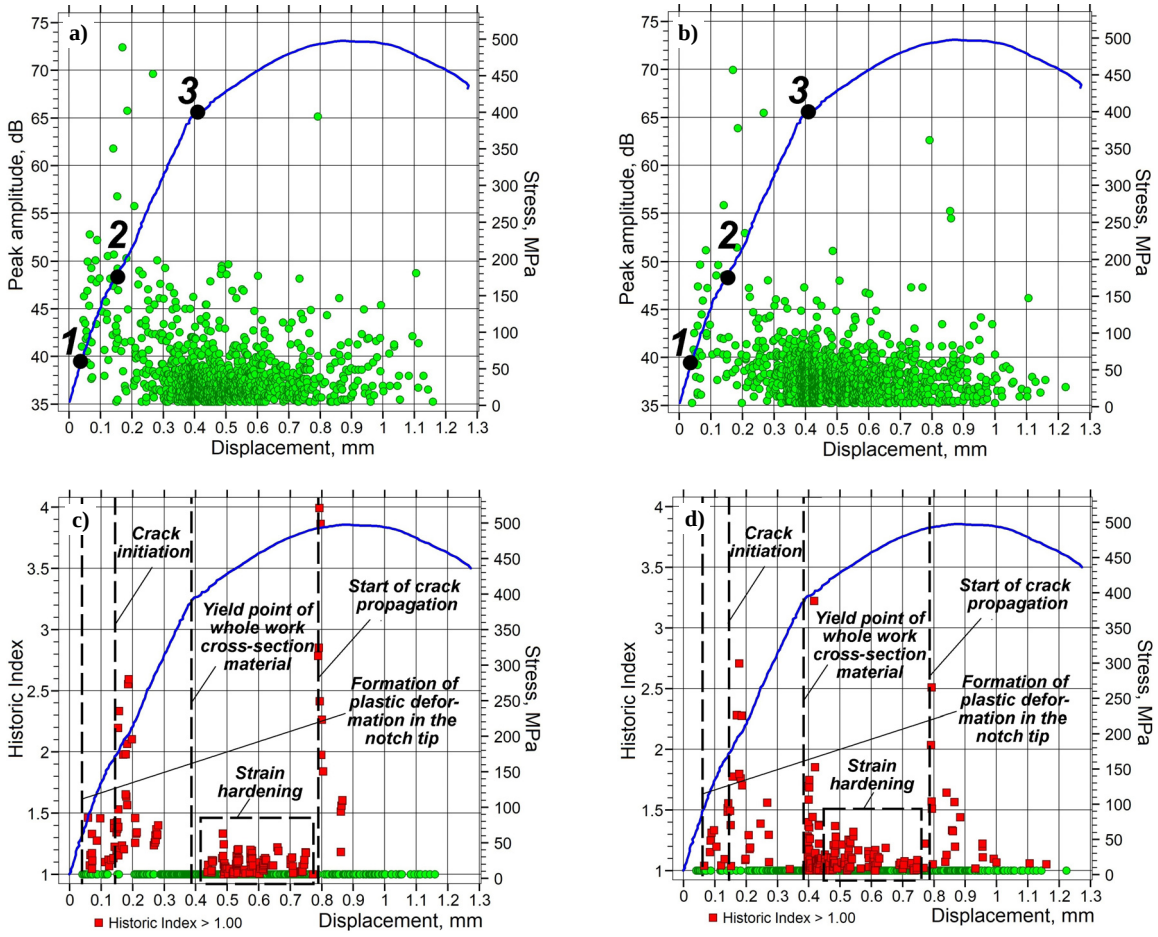

Fig. 6. Stress-displacement curves of 'S235-notched' type specimen with AE signal amplitude (a, b) and Historic Index signal parameter (c, d) distributions for type VS150-M sensors (a, c) and type VS75-V sensors (b, d) as well as von Mises stress distribution in work zone of the specimen (e-g) for different loading levels (points 1-3 on stress-displacement curves a and b)

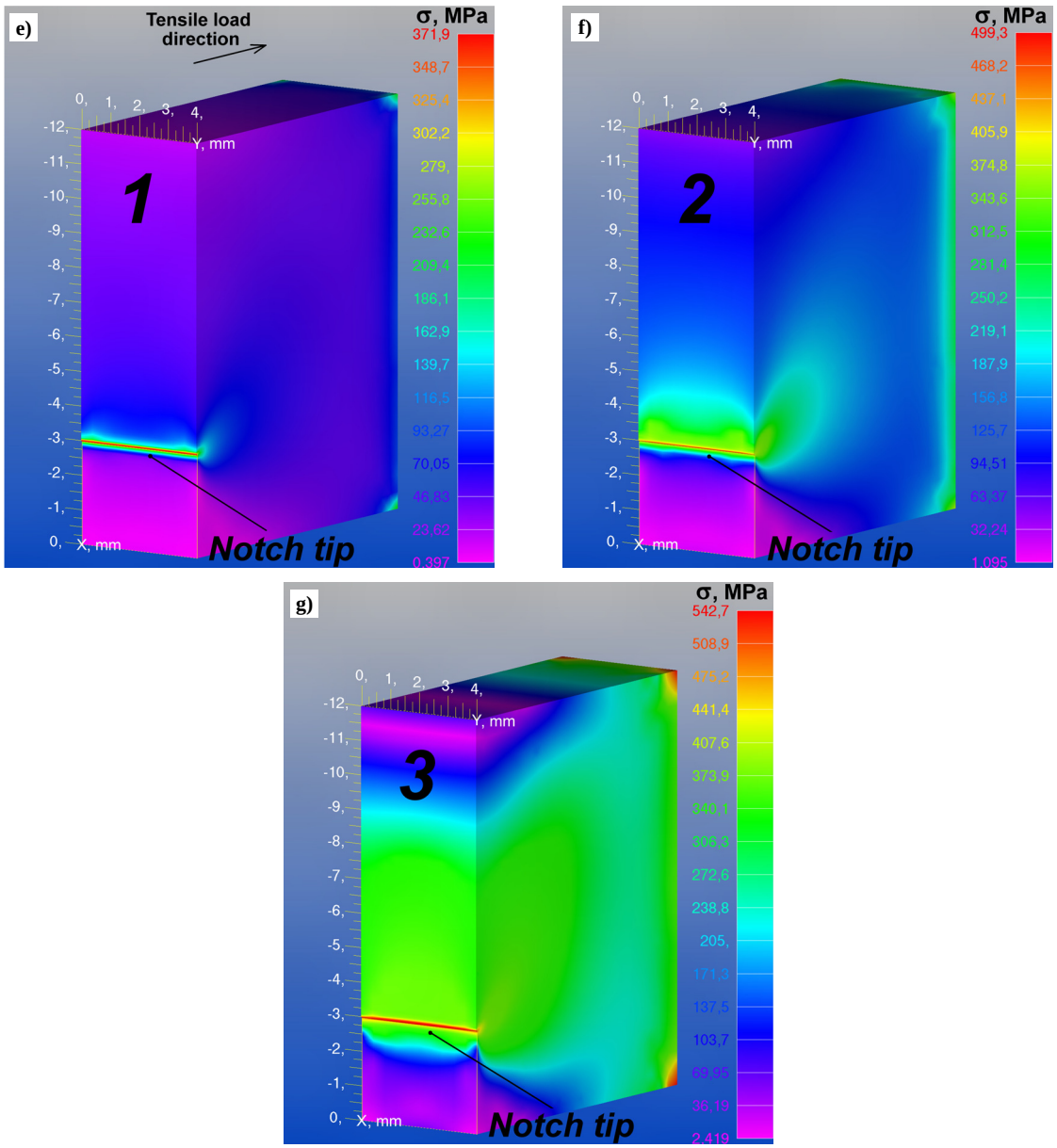

Fig. 6. Continued. Stress-displacement curves of 'S235-notched' type specimen with AE signal amplitude (a, b) and Historic Index signal parameter (c, d) distributions for type VS150-M sensors (a, c) and type VS75-V sensors (b, d) as well as von Mises stress distribution in work zone of the specimen (e-g) for different loading levels (points 1-3 on stress-displacement curves a and b)

3. The tested St3S grade carbon steel of a distillation column shell (after 50 years of operation) showed overheated microstructures. The steel microstructure was coarse-grained with sharp-shaped pearlite grains. These microstructural defects arose from improper normalisation treatment after hot rolling during steel plate manufacturing.
4. The maximum AE activity around the yield point on the stress-displacement curves of the unnotched samples was observed. It was found that AE at the early stage of plastic deformation, preceded by a yield point, is generated by dislocation movement – the intensive development of slip bands in plastic ferrite grains. The decrease of AE activity is observed during the strain hardening stage when the dislocations accumulate and serve as obstacles for their limited motion.
5. The micro-cracking process in the linear plastic deformation zones of ferrite grains, immediately before and after the maximum load, generates single burst signals with peak amplitudes of approx. 50-60 dB. The growth and linkage of both micro-crack and macro-crack formation are found in the final fracture stage.
6. The detailed analysis of parameters of AE signals generated during the tensile testing of notched specimens allowed the identification of each stage/mechanism of the deformation and fracture processes: material plastic deformation and crack initiation near the notch tip; deformation and strain hardening in the whole work cross section of specimens; stable crack growth.
7. It was as confirmed that AE sensors with a resonance frequency of 75 kHz were more sensitive to plastic defor-

mation of steel, but S150-M type sensors with a frequency of 150 kHz had a higher sensitivity to crack initiation and propagation processes.

Acknowledgements

The authors would like to thank dr hab. J. Schmidt, msc. eng. B. Kozub and msc. eng. T. Ryncarz for their help in the implementation of research. This study was supported by the project of the LIDER VII Programme financed by the National Centre for Research and Development of Poland.

REFERENCES

[1] A. Lazarev, A. Vinogradov, J. of Acoustic Emission **27**, 144-156 (2009).

[2] D.M. Almeida, N.S. Maia, A.Q. Bracarense, E.B. Medeiros, T.M. Maciel, M.A. Santos, Soldagem Insp. **12** (1), 55-62 (2007).

[3] M. Nowak, I. Lyasota, D. Kisała, Testing the node of railway steel bridge using an acoustic emission method, Advances in Acoustic Emission Technology: proceedings of the World Conference on Acoustic Emission-2015, Springer (2017).

[4] H.W. Wang, H.M. Yu, H.Q. Xiao, Z.Y. Han, H.Y. Luo, Materials Research Innovations **19**, 288-291 (2015).

[5] M. Marsudi, Study of acoustic emission during tensile test of mild steel plate, 8th International Conference on Heat Transfer, Fluid Mechanics and Thermodynamics, 11-13 July 2011 Mauritius.

[6] S. Zou, F. Yan, G. Yang, W. Sun, Data Analysis Sensors **17**, 1-13 (2017).

[7] M. Akbari, M. Ahmadi, Physics Procedia **3**, 795-801 (2010).

[8] D. Yang, L. Yang, F. Dong-Ming, J. Cent. South Univ. **21**, 3692-3697 (2014).

[9] E. Merson, A. Vinogradov, D.L. Merson, J. of Alloys and Compounds **645**, 460-463 (2015).

[10] Z. Penglin, S. Yuan, Z. Zhiqiang, X. Yaxing, J. of Gansu Sciences **2**, 83-87 (2015).

[11] D.L. Merson, E.V. Chernyaeva, Metal Science and Heat Treatment **49**, 272-276 (2007).

[12] C.S. Lee, J.H. Huh, D.M. Li and D.H. Shin, ISIJ International **39**, 365-370 (1999).

[13] Y. Zhang, Z. Wen, B. Li, H. Wu, Experimental research on acoustic emission characteristics in damage process of different meso-structural specimens, 2015 Symposium on Piezoelectricity, Acoustic Waves, and Device Applications, Oct. 30-Nov.2 2015 Jinan, China.

[14] P. Sędek, P. Gotkowski, J. Brózda, Arch. Metall. Mater. **55** (20), 553-562 (2010).

[15] A. Fallahi, R. Khamedi, G. Minak, A. Zucchelli, Materials Science and Engineering A **548**, 183-188 (2012).

[16] R. Khamedi, A. Fallahi, A. Refahi Oskouei, Materials and Design 31, 2752-2759 (2010).

[17] S.A. Nikulin, A.B. Rozhnov, A.V. Nikitin, V.G. Khanzhin, S.O. Rogachev, V. Yu. Turilina, V.I. Anikeenko, Metal Science and Heat Treatment **60**, 209-215 (2018).

[18] V.G. Khanzhin, M.A. Shtremel, Metal Science and Heat Treatment **51**, 250-255 (2009).

[19] S.A. Nikulin, V.G. Khanzhin, Metal Science and Heat Treatment **41**, 174-181 (1999).

[20] GOST 380-60 Common quality carbon steel. Grades.

[21] PN-EN 10025-2:2007 Hot Rolled Products of Structural Steels – Part 2: Technical Delivery Conditions for Non-Alloy Structural Steels.

[22] PN-EN 13554:2011 Non-destructive testing. Acoustic emission testing. General principles.

[23] K. Ohno, M. Ohtsu, Construction and Building Materials **24**, 2339-2346 (2010).

[24] T.J. Fowler, J.A. Blessing, P.J. Conlisk, T.L. Swanson, The MONPAC System, World Meeting on Acoustic Emission. Charloue. N. Carolina. March 1989.